Thermochimica Acta, 24 (1978) 315–325

ON THE USE OF ELECTRON PARAMAGNETIC RESONANCE TO IMPLEMENT THERMOGRAVIMETRY DATA: THE THERMAL DECOMPOSITION OF ZINC OXALATE DIHYDRATE*

ZELIMIR GABELICA** AND RENÉ HUBIN

Université de Liège au Sart-Tilman, Département de Chimie Générale et de Chimie Physique, Sart-Tilman, B-4000-par Liège I (Belgium)

ERIC G. DEROUANE***

Facultés Universitaires de Namur, Laboratoire de Catalyse, 61, rue de Bruxelles, B-5000-Namur (Belgium)

ABSTRACT

The complementary use of thermogravimetric analysis and electron paramagnetic resonance spectroscopy enables the identification on interrelated and successive steps in the vacuum decomposition of $ZnC_2O_4 \cdot 2H_2O$. After completion of the oxalate dehydration, CO adsorbed species (analoguous to those previously reported on MgO) are observed by EPR, starting at a temperature of 250°C. In the temperature range 250–350°C, the CO ad-species disappear while paramagnetic ZnO_{1-x} and possibly CO_4^- entities are formed. It is proposed that the latter stems from the reaction of oxygen released by the decomposition of ZnO with CO_2 produced during the oxalate decomposition. Above 300°C, ZnO_{1-x} and CO_4^- disappear, leading to the formation of O_3^{3-} centers. The latter are gradually decomposed between 350 and 575°C, releasing O_2 observed in EPR as O_2^- molecular anions and trapped electrons which are again detected as ZnO_{1-x}. A partially reduced ZnO phase is most probably the end-product of the decomposition.

INTRODUCTION

Recently, it has been shown that thermogravimetric analysis and electron paramagnetic resonance (EPR) measurements could be combined with great success for the elucidation of complex thermolysis mechanisms. This integrated approach was used in the study of the decomposition of oxalates[1] and chromate–oxalate mixtures[2, 3] for several alkaline-earth metals, i.e., Ba, Sr, and Mg.

---

* Presented at the 14th Conference on Vacuum Microbalance Techniques Salford, 27th–28th September 1976.

** Present address: Facultés Universitaires de Namur, Laboratoire de Catalyse.

*** To whom queries concerning this paper should be sent.

The present contribution extends our former work to the investigation of the decomposition of zinc oxalate for which many interesting phenomena are expected because of the peculiar properties of the reaction product. Indeed, it is well-known that ZnO, treated in reducing atmosphere[4] and even when heated under vacuum[5], looses part of its oxygen with the formation of non-stoichiometric ZnO_{1-x}. The latter is responsible for the formation of various paramagnetic species (electron excess or electron defect centers, respectively of F or S, or of V type) among which some have shown an interesting reactivity towards O_2[6], CO[7, 8], and CO_2. The last two molecular species being released during the decomposition of the oxalate to ZnO, it seemed to us that this system was particularly suitable for the investigation of the possible gas–solid reactions occurring during the decomposition of the oxalate and for the identification of the adsorbed, eventually paramagnetic, residues.

This work clears some of the various intermediate steps which occur during the thermolysis of zinc oxalate. Various adsorbed or lattice paramagnetic species are identified which can account partially for the observed non-stoichiometry of the reaction products.

EXPERIMENTAL PART

Preparation of the Zn oxalate

$ZnC_2O_4 \cdot 2H_2O$ has been prepared by double decomposition using Zn chloride and oxalic acid. The purity of the reaction product has been checked by X-ray diffraction and chemical analysis. The thermogravimetric analysis confirms the presence of two hydration water molecules.

Thermal analysis and EPR measurements

The procedures used for conducting the thermal decompositions and recording the EPR spectra are identical to those which have previously been reported[1–3].

RESULTS

The thermal analysis of the decomposition under vacuum ($p = 10^{-4}$ torr) and in air of $ZnC_2O_4 \cdot 2H_2O$ confirms previously published results[9, 10]. The decomposition occurs following the scheme:

$$ZnC_2O_4 \cdot 2H_2O_{(s)} \rightarrow ZnC_2O_{4(s)} + 2\,H_2O_{(g)} \qquad 65\text{–}120\,^{\circ}C\ (125\text{–}175\,^{\circ}C) \qquad (1)$$

$$ZnC_2O_{4(s)} \rightarrow ZnO_{(s)} + CO_{(g)} + CO_{2(g)} \qquad 290\text{–}360\,^{\circ}C\ (340\text{–}410\,^{\circ}C) \qquad (2)$$

$$ZnO_{(s)} \rightleftarrows Zn_{(s)} + 0.5\,O_{2(g)} \qquad T > 290\,^{\circ}C \qquad (3)$$

where the subscripts (s) and (g) refer respectively to solid and gaseous compounds. The temperatures indicated are for the vacuum decomposition; values in parentheses correspond to the decomposition in air. Results are shown in Fig. 1.

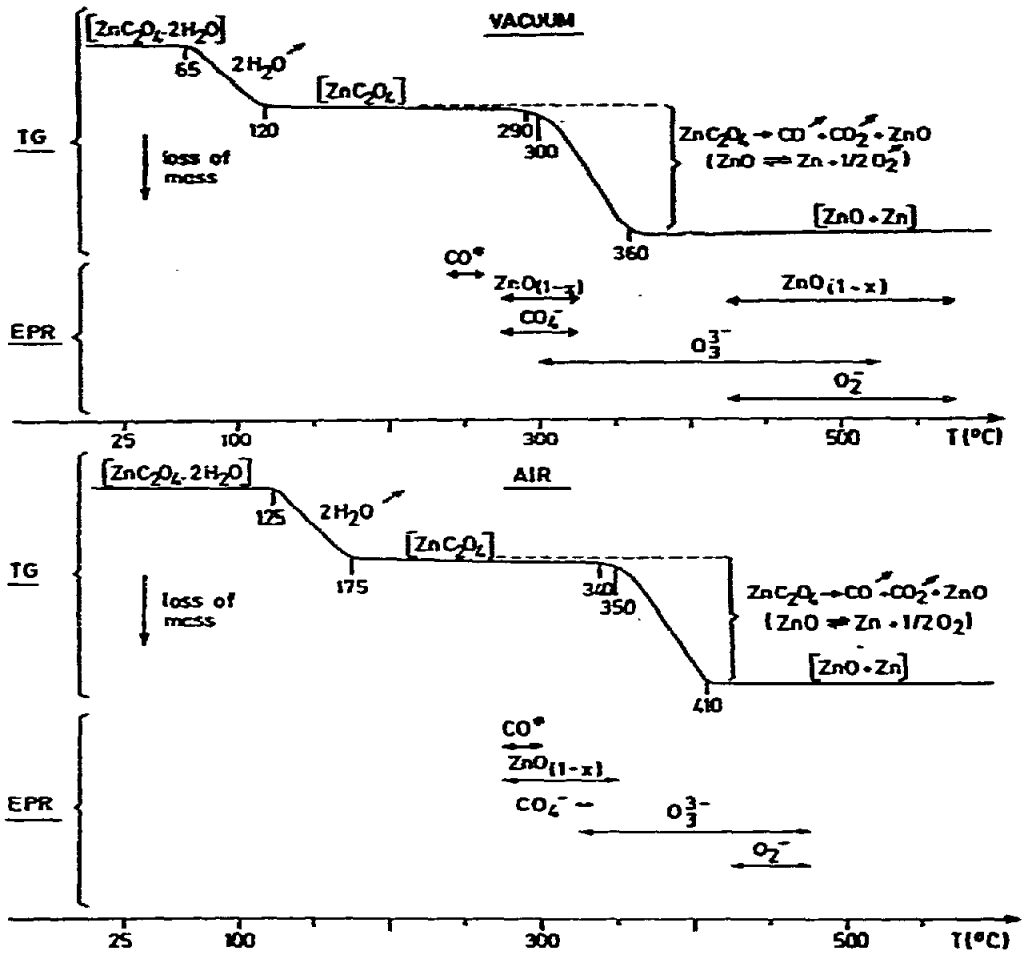

Fig. 1. Thermal analysis data for the decomposition of $ZnC_2O_4 \cdot 2H_2O$ under vacuum and in air. TG = Thermogravimetric measurements; EPR = electron paramagnetic resonance data; signals as indicated.

Between 120 and 290°C for the vacuum decomposition (175–340°C for the thermolysis in air), the thermal analysis curve presents a slight slope which corresponds to the last stage in the dehydration of the oxalate and the beginning of its decomposition with some release of CO and CO_2.

For the decomposition under vacuum, the observed weight loss between 290 and 360°C is somewhat larger than the calculated value assuming process (2). The difference is attributed to a partial reduction of ZnO (according to reaction (3)) as has been suggested previously[9, 10].

The use of EPR enables the identification of several different radical species formed in steps (2) and (3). Some of these will be identified as adsorbed gaseous residues, others as surface centers belonging to the ZnO lattice, thereby providing a more detailed description of the chemical reactions occurring at the various temperatures.

Five different paramagnetic species are formed and observed, either simul-

TABLE I

EPR SIGNALS OBSERVED DURING THE THERMOLYSIS OF ZINC OXALATE AND THEIR INTERPRETATION

Signal	*g-values*	*Interpretation*
A	$g_{\perp} = 2.0052$; $g_{//} = 2.0024$ $g_{iso} = 2.0043$	$CO^*_{(ads)}$
B	$g = 1.96$	ZnO_{1-x}, trapped e^-, or Zn^+.
C	$g_1 = 2.0428$, $g_2 = 2.0088$, $g_3 = 2.003$	CO_4^-
D	$g = 2.0033$	O_3^{2-} or V_I
E	$g_1 = 2.0448$, $g_2 = 2.0081$, $g_3 = 2.0026$ $g_{iso} = 2.0185$	O_2^-

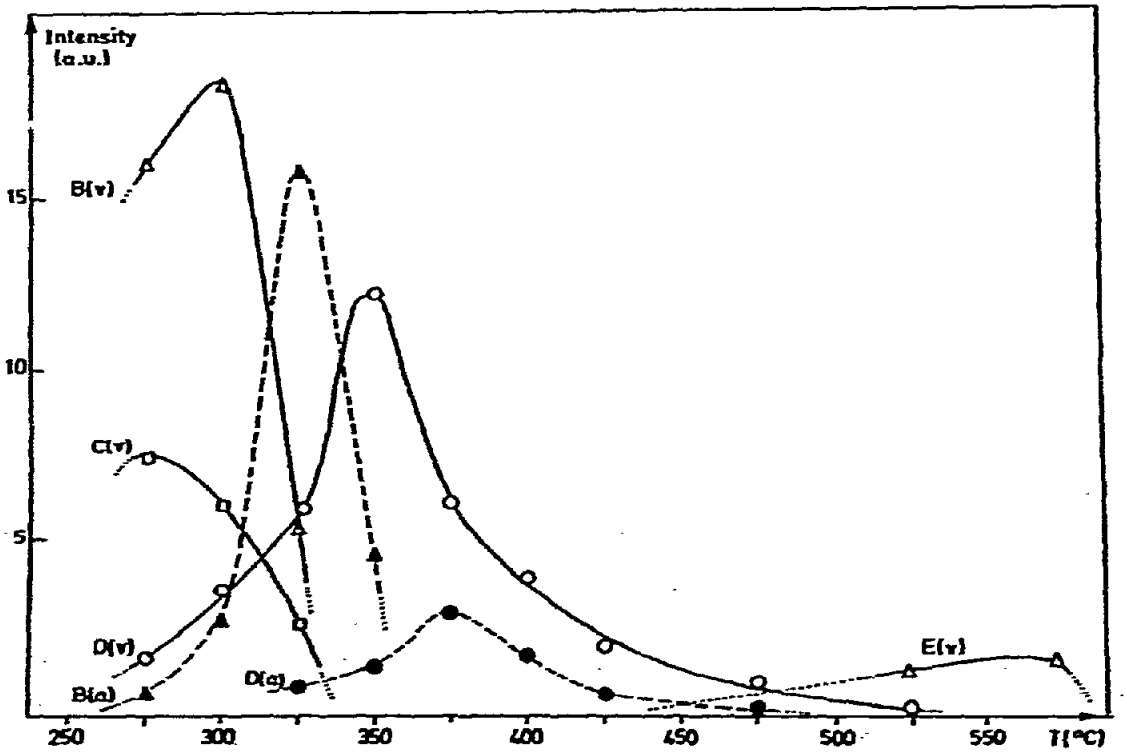

Fig. 2. Intensity variation of the various EPR signals as a function of temperature: (v) under vacuum, (a) in air.

taneously or in succession as shown in Table 1. A plot of their intensities, as a function of temperature, is given in Fig. 2.

Signal A is asymmetrical (Fig. 3) with g-values respectively equal to $g_{//} = 2.0024$ and $g_{\perp} = 2.0052$ (isotropic g-value, $g_{iso} = 2.0043$). It appears at about 250°C. Its characteristics are very close to those of the excited CO^* radical adsorbed on MgO[1, 7]. It is a neutral, or slightly positive, CO species in an excited electronic state. Its g-values are listed and compared to literature data in Table 2.

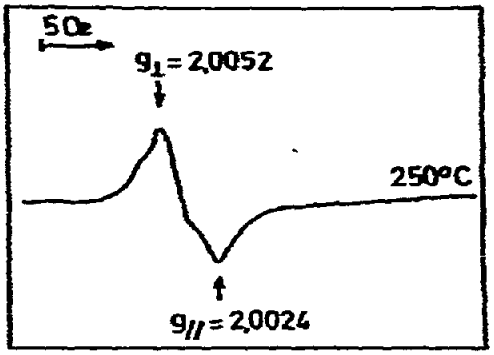

Fig. 3. EPR spectrum of signal A, CO^*, as observed after activation at 250°C.

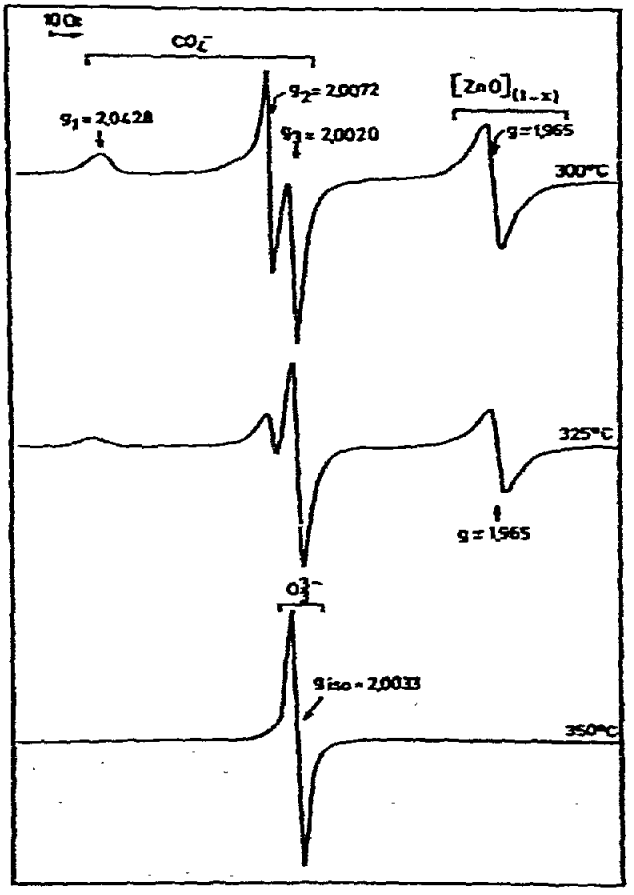

Fig. 4. EPR spectra of Zn oxalate after vacuum activation at 300, 325, and 350°C, showing signals B, C, and D.

Signal B, as shown in Figs. 4 and 5 is almost isotropic. It has a g_{iso} value of about 1.96 which depends to some extent on the thermal treatment temperature (275–325°C and 425–575°C). The lower than the free electron g_{iso} value indicates that we deal with an electron excess paramagnetic center. This signal is almost always

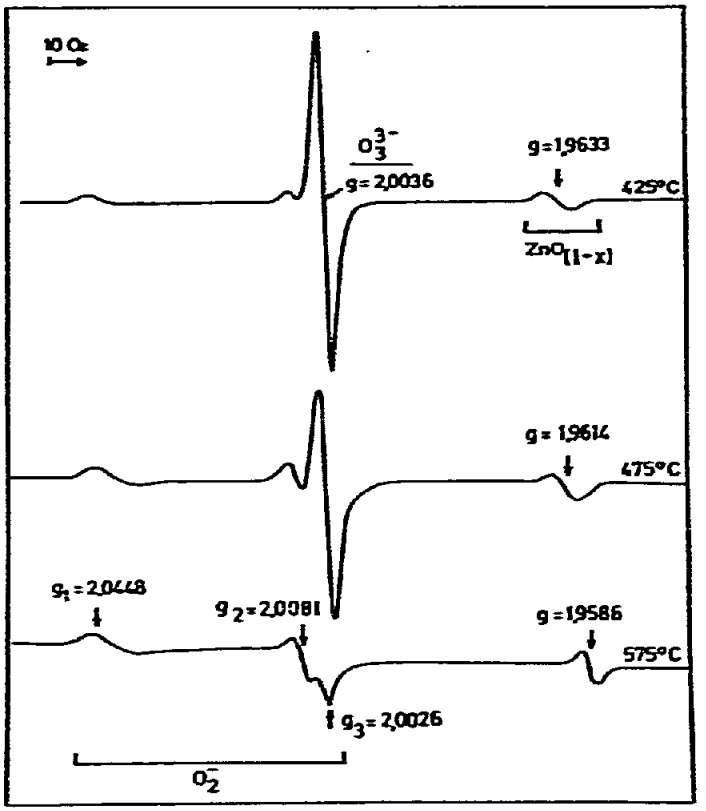

Fig. 5. EPR spectra of Zn oxalate after vacuum activation at 425, 475, and 575°C, showing signals B, D, and E.

TABLE 2

g-VALUES OF CO RADICALS ON MgO AND ZnO

Precursor	$g_{\parallel}$	$g_{\perp}$	g_{iso}	*Ref.*
^{13}CO, gas, MgO	2.0021	2.0055	2.0043	7
^{12}CO, decomp. Mg oxalate	2.0026	2.0051	2.0043	1
^{12}CO, decomp. Zn oxalate	2.0024	2.0052	2.0043	This work

observed in irradiated ZnO and various interpretations of its nature have been proposed. The most recent reports however agree to attribute this signal to an electron more or less bound to a Zn^{2+} ion[11] although the detailed structure of this species is still unknown. It could be Zn^+, F centers, conduction electrons, or even interstitial Zn... The observation by Hausmann[12] of an hyperfine structure due to ^{67}Zn in the EPR spectrum of this species confirms the general picture that Zn^{2+} ions act as acceptors, the electron being partially localized on Zn. We will then represent the paramagnetic species responsible for signal B at $g = 1.96$ by Zn^+, (e^-), or more

TABLE 3

VARIATION OF THE g-VALUE OF SIGNAL (B) AS A FUNCTION OF ACTIVATION TEMPERATURE

Temp. (°C)	*g-value*
275–325	1.965
425	1.963_2
475	1.961_4
575	1.958_6

TABLE 4

g-VALUES OF SIGNAL (C) AND OF VARIOUS OXYGEN-CONTAINING RADICALS

Radical	*Formation*	*g-values*				*Ref.*
		g_1	g_2	g_3	g_{iso}	
(C)	Decomp. ZnC_2O_4	2.0428	2.0088	2.003	2.0182	This work
CO_3^-	$O_3^{3-} + CO \rightarrow O^{2-} + CO_3^-$	2.0465	2.006	2.001	2.0178	15
O_2^-	$O_2 + h\nu \rightarrow O_2^-$	2.050	2.008	2.003	2.0203	6
CO_4^-	$CO_2^- + O_2 \rightarrow CO_4^-$	2.040	2.0072	2.002	2.0164	13

generally by (ZnO_{1-x}). The variation of its g-value with temperature is given explicitly in Table 3.

Signal C is highly asymmetrical (Fig. 4 and Table 4) and it is observed after thermal treatments conducted between 275 and 325°C. The data shown in Table 4 indicate that this signal is rather identical to that recently[13] attributed to CO_4^-. Moreover, as it will be seen in the discussion, its identification to the latter species enables to propose a mechanism accounting for the apparition, progressive changes and disappearance of the other signals which are also observed and attributed to intermediate species.

An isotropic signal with g_{iso}-value equal to 2.0033 is found to be present in the temperature range 275–575°C. It will be referred to as signal D as indicated in Figs. 4 and 5. It is characteristic of the V_1, or O_3^{3-} species, as observed on MgO[3, 14], ZnO[11] and possibly TiO_2[15].

Finally, at higher temperature (425–575°C), one can also note the presence of a weak asymmetrical signal (referred to as E) with g-values $g_1 = 2.0448$, $g_2 = 2.0081$, and $g_3 = 2.0026$. As seen from Table 4, these values characterize the molecular anion O_2^-.

If the thermal decomposition is conducted in air, similar signals are observed. The major differences are their relative intensities and their apparition and disappearance temperatures. The discussion will deal almost exclusively with the results of the vacuum decomposition experiments.

TABLE 5

SUMMARY OF THE OBSERVATIONS AND THEIR INTERPRETATION FOR THE DIFFERENT STEPS DURING THE THERMOLYSIS OF ZINC OXALATE DIHYDRATE

Step	*Temp. (°C)*	*Thermal analysis data*		*EPR data*	
		Observed	*Interpretation*	*Observed*	*Interpretation*[a]
1	<250	H_2O release	—	—	—
2	250			signal A	4
3	250–300	Release of CO and CO_2	Reactions (2) and (3)	signal A disappears	6
				signal B	5, 7
				signal C	9, 9′
4	300–350	Release of CO and CO_2	Reactions (2) and (3)	signal B	8, 8′
				signal C	10
				signal D	10
5	350–575	Release of CO and CO_2	Reactions (2) and (3)	signal D	11
				signal E increases and then disappears	11
				signal B reappears and decreases	12

[a] Numbers refer to reactions as indicated in text.

DISCUSSION

The combined use of the thermal analysis data and of the EPR measurements, as a function of the decomposition temperature, enable the distinction of five successive steps which characterize the thermolysis under vacuum as evidenced by Table 5.

The first step certainly is the dehydration of the oxalate which is completed at about 120°C. No EPR signal is observed below 250°C.

At 250°C, EPR shows the presence of adsorbed CO radical species produced by the chemisorption of CO released during some partial decomposition of the oxalate:

$$CO_{(g)} \rightarrow CO^{\bullet}_{(ads)} \qquad (4)$$

as also evidenced by a small weight loss before the real start of the decomposition.

The thermogravimetric curve shows that release of CO and CO_2 occurs between 250 and 300°C. Important changes occur in the EPR spectra from and above that temperature. The CO* signal disappears while two new signals appear which are attributed to CO_4^- and ZnO_{1-x} (trapped electrons). The latter species (ZnO_{1-x}) stems probably from a partial decomposition of the freshly produced oxide. Gaseous (or adsorbed) oxygen can then react with CO* with formation of CO_2 and disappearance of the CO* EPR signal:

$$ZnO \rightarrow ZnO_{1-x} + x/2\, O_2 \quad (5)$$

$$x\, CO^{*}_{(ads)} + x/2\, O_2 \rightarrow x'\, CO_{2(g)} + x''\, CO_{2(ads)} \quad (6)$$

corresponding to the overall reaction:

$$ZnO + x\, CO^{*}_{(ads)} \rightarrow ZnO_{1-x}\,(\text{or } e^-) + x'\, CO_{2(g)} + x''\, CO_{2(ads)} \quad (7)$$

In a recent paper[1], we have shown that the adsorbed CO* species, on MgO, was stable at temperatures much higher than 300°C. Hence, it confirms that in the present case, the disappearance of the adsorbed CO species must be due to a real chemical reaction of CO* with one or more of the reaction products and not to a simple desorption phenomenon. In addition, steps (5) and (6) explain the simultaneous apparition of CO_2 and O_2 at the surface of the solid residue. Molecular oxygen produced by (5) can trap electrons from ZnO_{1-x} species (signal B) and react with CO_2 formed during step (6) leading to CO_4^- species.

The mechanism would be as follows:

$$(e^-) + O_2 \rightarrow O_2^- \quad (8)$$

$$O_2^- + CO_{2(g \text{ or ads})} \rightarrow CO_{4(ads)}^- \quad (9)$$

another possibility being:

$$(e^-) + CO_{2(g)} \rightarrow CO_{2(ads)}^- \quad (8')$$

$$CO_{2(ads)}^- + O_2 \rightarrow CO_{4(ads)}^- \quad (9')$$

No EPR signal characteristic of $CO_{2(ads)}^-$ is observed (contrarily to the case of MgO[1]) and hence, if present, it should have a lifetime smaller than 10^{-10} sec. This gives further support to steps (9) and (9') in which CO_2 intermediates immediately react with oxygen.

Starting from 300°C, the intensities of signals B and C decrease rapidly. They have completely vanished at 325°C and a new species, O_3^{3-}, appears. The disappearance of the CO_4^- and of the ZnO_{1-x} species with the formation of O_3^{3-} can be explained by a mechanism which involves the participation of one oxygen atom from the ZnO lattice:

$$CO_{4(ads)}^- + O^{2-}_{(lattice)} \rightarrow CO_{2(g)} + O_3^{3-} \quad (10)$$

The disappearance of CO_4^- must lead to the disappearance of ZnO_{1-x} which was its precursor. CO_2 is released as it cannot adsorb on the acidic (electron defect) site O_3^{3-} (V_I).

Between 350 and 575°C, the intensity of the O_3^{3-} signal decreases steadily and two new paramagnetic species can be identified: the previously reported ZnO_{1-x} (or e^- trapped on Zn^{2+}) with a small intensity and mainly the oxygen molecular anion O_2^-. From these results, we then have some evidence for the occurrence of the following processes:

$$O^{3-}_{3(ads)} \rightarrow O^{2-} + O^{-}_{2(ads)} \quad (11)$$

$$O^{-}_{2(ads)} \rightarrow O_{2(g)} + ZnO_{1-x}\,(\text{or } e^{-}) \quad (12)$$

No EPR signal is observed above 575°C. The X-ray diffraction diagram confirms that the end-product is ZnO but does not show traces of partial reduction (such as the presence of metallic Zn, eventually) although the latter is apparent from the thermogravimetric data.

CONCLUSIONS

The combination of thermal analysis measurements and of EPR data has enabled to propose a detailed mechanism of the various reactions which occur during the thermal decomposition in vacuum of zinc oxalate dihydrate.

The successive reactions scheme represented in Fig. 6 summarizes the observations and our conclusions, showing the important role played by non-stoichiometric and intermediate phases. It is emphasized that although the decomposition of this compound is certainly a solid-state reaction, gas–solid and/or gas–surface reactions play a major role.

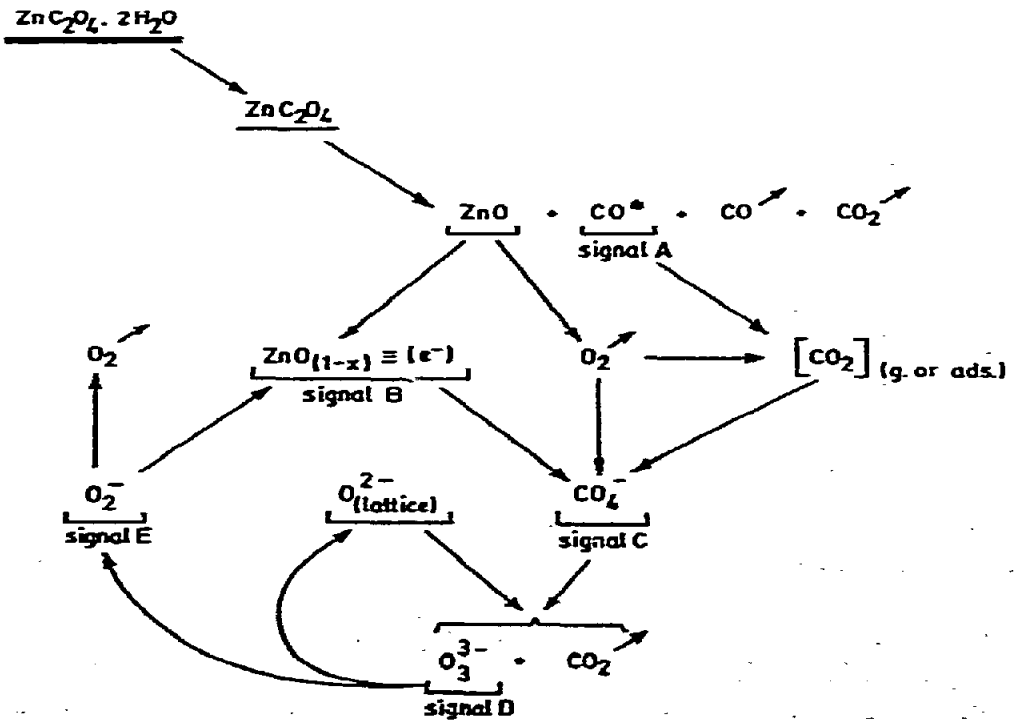

Fig. 6. Summary of the successive reactions, as identified by EPR, occurring during the thermolysis of Zn oxalate.

REFERENCES

1 E. G. Derouane, Z. Gabelica, R. Hubin and M. J. Hubin-Franskin, *Thermochim. Acta*, 11 (1975) 287.
2 E. G. Derouane, Z. Gabelica and R. Hubin, *Thermochim. Acta*, 14 (1976) 315.
3 E. G. Derouane, Z. Gabelica and R. Hubin, *Thermochim. Acta*, 14 (1976) 327.
4 F. Steinbach, *Z. Phys. Chem. N.F.*, 60 (1968) 126.
5 A. Cimino, E. Molinari and F. Cramarossa, *J. Catal.*, 2 (1963) 315.
6 J. H. Lunsford and J. P. Jayne, *J. Chem. Phys.*, 44 (1966) 1487.
7 J. H. Lunsford and J. P. Jayne, *J. Chem. Phys.*, 44 (1966) 1492.
8 K. M. Sancier, *J. Catal.*, 9 (1967) 331.
9 R. David, *Bull. Soc. Chim. Fr.*, (1960) 719.
10 K. Nagase, K. Sato and N. Tanaka, *Bull. Chem. Soc. Jpn.*, 48 (1975) 439.
11 Ning-Bew Wong, Y. Ben Taarit and J. Lunsford, *J. Chem. Phys.*, 60 (1974) 2148.
12 A. Hausmann, *Z. Phys.*, 237 (1970) 86.
13 Y. Ben Taarit, P. Mériaudeau, J. C. Védrine, C. Naccache and Ph. De Montgolfier, *J. Chem. Phys.*, 67 (1977) 2880.
14 M. Boudart, A. J. Delbouille, E. G. Derouane, V. Indovina and A. B. Walters, *J. Am. Chem. Soc.*, 94 (1972) 6622.
15 P. Mériaudeau and J. C. Védrine, *J. Chem. Soc. Faraday*, 72 (1976) 472.